# Production of $H_2$ by Ethanol Photoreforming on $Au/TiO_2$

*Alberto V. Puga, Amparo Forneli, Hermenegildo García, and Avelino Corma**

**A deposition-precipitation method is used to prepare $Au/TiO_2$ solids (0.45–1.7 wt% Au). These materials, consisting of gold nanoparticles (diameter range = 1.5–6.5 nm) supported on the surface of $TiO_2$, are used as photocatalysts for the ethanol photoreforming reaction under either UV-rich or simulated solar light. The main products of such reactions are $H_2$ in the gas phase and acetaldehyde in the liquid phase according to the reaction $CH_3CH_2OH \rightarrow CH_3CHO + H_2$. Among the gaseous products, $H_2$ amounts to around or above 99% in all cases; other minor products found in the gas phase are, in decreasing order of molar production: $CH_4 > CO > C_2H_4 > CO_2 > C_2H_6 > C_3H_8$. The photoactivity is lower under $CO_2$ atmosphere, as compared to analogous reactions performed under Ar. The $H_2$ production yields are very high (up to a maximum 30 mmol $g_{cat}^{-1}$ $h^{-1}$) under UV irradiation, and increase with increasing gold loading. The reactions under simulated solar light also yield significant amounts of $H_2$ (5–6 mmol $g_{cat}^{-1}$ $h^{-1}$) as the main gaseous product.**

## 1. Introduction

The efficient use of solar light as the energy source for chemical transformations would certainly be an advantageous technology for the production of renewable fuels, e.g. $H_2$ from water splitting[1] or $CH_4$ or methanol from $CO_2$ reduction.[2] Nevertheless, the efficiency of such processes is not as high as desirable from an economical perspective. Given the limited tendency of water itself to be oxidised to $O_2$, the production of $H_2$ from water can be promoted by the use of sacrificial electron donors.[1] Among these, organic substances such as alcohols have proven useful, although at the expense of their consumption in the process. For example, methanol or ethanol are oxidised primarily to formaldehyde[1,3] or acetaldehyde,[4] respectively, a process that can be considered alcohol photoreforming. Notwithstanding this, processes of this kind, which enable the conversion of organic substances with concomitant $H_2$ release by means of light, are of significant practical interest, not only due to the production of $H_2$, but also when coupled with the photo-oxidation of organic pollutants from aqueous streams.[1,4] Such reactions are carried out under inert atmospheres, generally under Ar, in order to avoid the competition of $O_2$ with the reduction processes; in this regard, it would be worth testing analogous reactions under $CO_2$, since coupling its reduction with alcohol oxidation would have practical interest.

In addition to photocatalytic reactions, a large variety of processes to produce $H_2$ from organic matter are known. In some cases, the organic feedstock is treated under harsh temperature and pressure conditions in the presence of steam and/or $O_2$; coal or biomass gasification are examples of this.[5] Recently, the aqueous phase reforming of biomass-derived organic matter has emerged as an interesting alternative,[6] given that it is less energy intensive as compared to previously known reforming processes. For example, methanol can be converted into a $H_2$-rich (albeit containing up to 25% $CO_2$ by volume) gaseous stream.[6a]

The potential of alcohol photoreforming, as compared to other reforming processes, lies in the fact that it may enable the production of $H_2$ at high rates and high purities by using solar light as the only energy source. In 1980, Kawai and Sakata reported that irradiation of suspensions of $Pt/TiO_2$ or $RuO_2$-$Pt/TiO_2$ solids in methanol/water mixtures with a Xe lamp (500 W) yielded $H_2$ at high rates, whereas $CO_2$ was also released.[3] Related to those investigations, it was also discovered that $H_2$ could be produced under similar conditions from aqueous suspensions or solutions of a wide range of biomass-derived substances, including sugars, starch or cellulose,[7] algae, wood, grasses or ethanol.[8] Later, Haruta and co-workers studied the activity of metal-loaded $TiO_2$ photocatalysts under Hg lamp light and concluded that both $Pt/TiO_2$ and $Au/TiO_2$ promote the release of $H_2$ from aqueous ethanol with high selectivities (94–97%, as estimated from the reported data) over $CH_4$ and $CO_2$.[4] Recently, the interest in using ethanol as the feedstock to obtain $H_2$ by photoreforming has increased. It has been confirmed that solids based on metal nanoparticles deposited on titania are highly efficient for such a purpose. Different films of $metal/TiO_2$ supported on glass were tested under UV light irradiation of ethanol/water mixtures, revealing that Pt was slightly more active than Au under those conditions.[9] The use of bimetallic $Pt\text{-}Au/TiO_2$ proved beneficial for the continuous $H_2$ evolution for several hours from aqueous ethanol under either UV-rich (Hg lamp) or simulated solar light.[10] Other catalysts displaying activity in similar systems, under either UV or visible light, are $Cu/TiO_2$,[11] $Pd\text{-}Au/TiO_2$[12] or various $M/TiO_2$ (M = Pt, Rh, Pd or Ni; $TiO_2$ = rutile).[13] Regarding $Au/TiO_2$ structure and morphology, recent studies have concluded

Dr. A. V. Puga, A. Forneli, Prof. H. García, Prof. A. Corma
Instituto Universitario de Tecnología Química CSIC-UPV
Universidad Politécnica de Valencia
av. de los Naranjos s/n, 46022, Valencia, Spain
E-mail: acorma@itq.upv.es

DOI: 10.1002/adfm.201301907

that anatase is considerably more active than rutile and that higher surface availability of Au is beneficial to $H_2$ production from ethanol under UV (350 nm) light,[14] although significant amounts of other gases (mostly CO, $CO_2$ and $CH_4$) are also released, probably by further photo-induced decomposition reactions.[14a]

The application of biomass photoreforming for the economical production of $H_2$ would only be a realistic possibility if solar energy could be used and if downstream separation could be minimised. The present work reports on the photocatalytic production of $H_2$ (≈ 99% of all gaseous products) from ethanol, a chemical derived from biomass in the industry. Comprehensive analyses of the products of such reactions under either UV-rich or simulated solar light have been conducted. The photocatalysts used were Au/$TiO_2$ solids, consisting of gold nanoparticles supported on anatase-rich titania. Similar Au/$TiO_2$ materials, prepared by deposition-precipitation methods, have proved to be highly valuable as photocatalysts for a number of reactions.[15] The effects of different gaseous atmospheres or different catalyst compositions (or absence of catalysts) have been explored, aiming at achieving yield enhancements and a certain degree of mechanistic understanding.

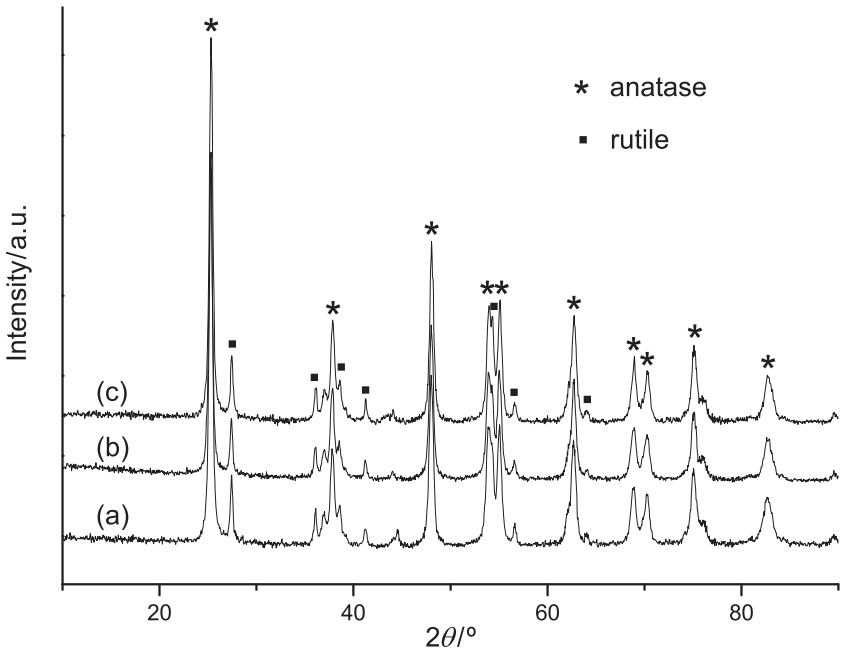


**Figure 1.** Powder X-ray diffractograms (Cu-$K_\alpha$, 0.154056 nm) for various Au/$TiO_2$ solids and for the pristine $TiO_2$: (a) $TiO_2$, (b) 0.45% Au/$TiO_2$, (b) 0.57% Au/$TiO_2$.

## 2. Results and Discussion

### 2.1. Synthesis and Characterisation of the Au/$TiO_2$ Photocatalysts

The Au/$TiO_2$ photocatalysts used in this work were prepared by a simple deposition-precipitation method, by using commercial P25 titania as support. The deposition stage was performed in aqueous solution at pH = 9 and with $HAuCl_4$ as the gold precursor. After separating the gold-deposited solids by filtration and washing with water, they were treated under $H_2$ at 300 °C to yield solid samples exhibiting purple colouration, indicative of the presence of gold nanoparticles. This synthetic method is similar to other well known procedures for producing photocatalytic Au/$TiO_2$ materials.[14,15]

The crystallinity of the Au/$TiO_2$ samples prepared was studied by powder X-ray diffraction (XRD) measurements. The diffractograms shown in **Figure 1** reveal that titania occurs as a mixture anatase and rutile phases in Au/$TiO_2$. The relative abundance of such crystalline phases is estimated as *ca.* 80/20%, which is essentially equal to that found for the pristine $TiO_2$ support (see Figure 1), thus leading to the conclusion that the structure of titania did not undergo significant changes throughout the synthetic processes, neither during the deposition-precipitation stages nor during the thermal reductive treatments with $H_2$. Due to the low gold contents and small particle sizes, no diffraction events ascribable to crystalline Au were observed.

Transmission electron microscopy (TEM) observations showed that the Au/$TiO_2$ photocatalysts consisted of titania particles (20–30 nm diameter) with smaller deposited gold nanoparticles, as expected. Furthermore, the gold nanoparticles were well dispersed on the titania surface, i.e. no abnormally large particles or aggregates were observed. The sizes of gold nanoparticles were measured from TEM micrographs (see an example for a 1.0% Au/$TiO_2$ sample in **Figure 2**). A statistical analysis of the sizes of gold nanoparticles was performed and a histogram showing the size distribution profile is shown in

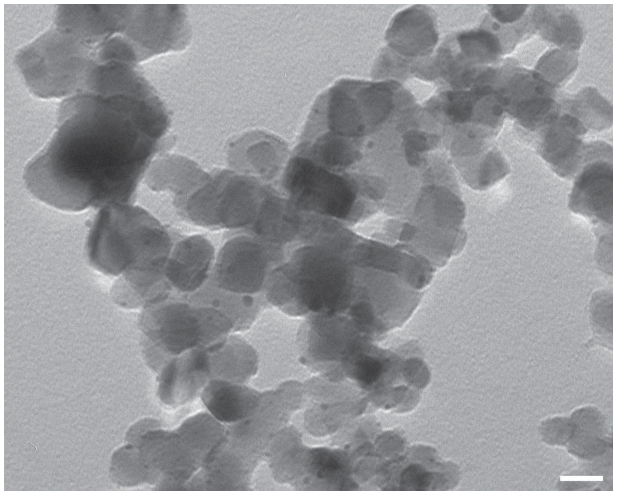

**Figure 2.** TEM micrographs (100 kV) recorded for a sample of 1.0% Au/$TiO_2$, where the larger particles of $TiO_2$ and the deposited Au nanoparticles can be observed. Scale bar: 20 nm.

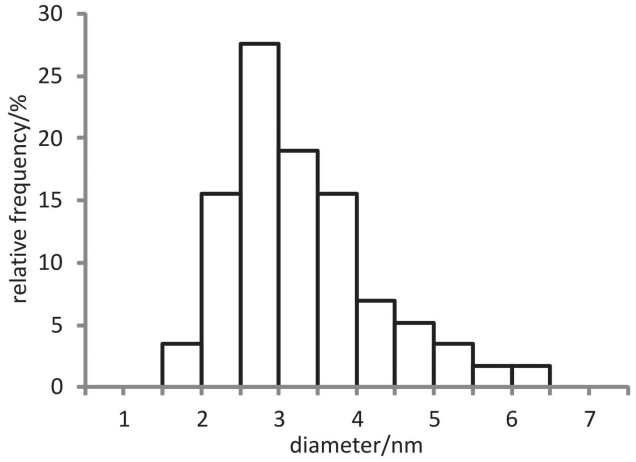


**Figure 3.** A histogram showing the Au nanoparticle size distribution for a sample of 1.0% $Au/TiO_2$, obtained by counting sixty individual particles.

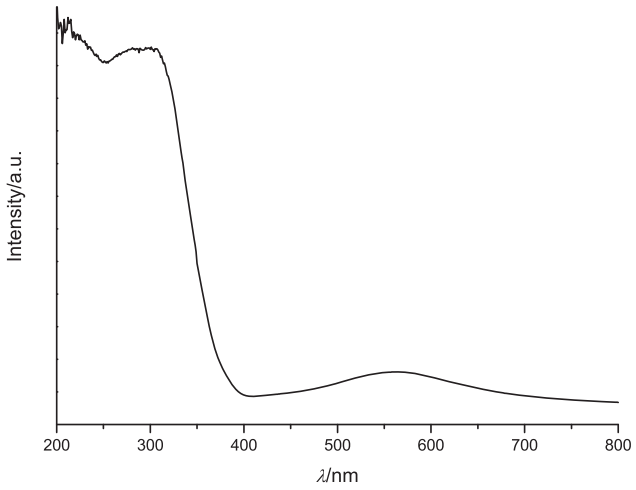


**Figure 4.** Diffuse reflectance UV-vis absorption spectra for 0.45% $Au/TiO_2$. The broad absorption band in the visible region (maximum at 563 nm) is attributable to the surface plasmon band of gold nanoparticles, whereas the intense band below 380 nm is due to the absorption of the $TiO_2$ semiconductor.

**Figure 3**. As can be seen therein, the diameters of Au nanoparticles range from 1.5 to 6.5 nm, with a maximum occurrence between 2.5 and 3.0 nm. Therefore, the deposition-precipitation synthetic method used in this work yields $Au/TiO_2$ materials consisting of evenly distributed small gold nanoparticles supported on titania surfaces. Such morphologies should confer photoactivity to the materials.

The nanometer-sized gold nanoparticles are known to exert visible-light absorption, a phenomenon which is due to the surface plasmon resonance.[15a] For the $Au/TiO_2$ samples reported herein, the aforementioned visible-light absorption was observed by diffuse reflectance UV-visible spectroscopy measurements. The spectrum shown in **Figure 4** confirms that the samples absorb in the visible region, with a maximum absorbance at 563 nm. In addition, the semiconducting characteristics of $TiO_2$ are responsible for intense UV light absorption, which in this case is clearly noticeable below 380 nm, therefore effectively covering the entire UV range. The combination of visible and UV light absorption by gold nanoparticles and titania, respectively, is known to enable photocatalytic activity on $Au/TiO_2$ surfaces. This is experimentally proven in this work by testing the prepared $Au/TiO_2$ materials for ethanol photoreforming processes.

### 2.2. Photocatalytic $H_2$ Generation from Ethanol Under Ar

The photocatalytic $H_2$ generation from ethanol with a Hg lamp under Ar on $Au/TiO_2$ solids resulted in the production of $H_2$, CO, $CO_2$ and hydrocarbons which accumulated in the gas phase, whereas the main product found in the liquid phase was acetaldehyde (data compiled in **Table 1**). Gaseous products are formed, from larger to smaller molar amounts, in the following

**Table 1.** Product yields for the photocatalytic ethanol reforming under UV-rich light on $Au/TiO_2$.[a)]

| | Gas | Solvent | Photocatalyst | Production rate [μmol $g_{cat}^{-1}$ $h^{-1}$] | | | | | | | | |
|---|---|---|---|---|---|---|---|---|---|---|---|---|
| | | | | Gas phase | | | | | | | Liquid phase | |
| | | | | $H_2$ | $CH_4$ | $C_2H_4$ | $C_2H_6$ | $C_3H_8$ | CO | $CO_2$ | $CH_3CHO$ | $CH_3COOH$ |
| **1** | Ar | EtOH | 0.45% $Au/TiO_2$ | 23180 | 78 | 32 | 6 | 1 | 51 | 19 | 23954 | – |
| **2** | Ar | EtOH | 0.57% $Au/TiO_2$ | 21152 | 71 | 32 | 8 | – | 40 | 73 | 19840 | 50 |
| **3** | Ar | EtOH | 1.0% $Au/TiO_2$ | 28542 | 109 | 45 | 7 | 1 | 57 | 22 | 28626 | – |
| **4** | Ar | EtOH | 1.7% $Au/TiO_2$ | 29677 | 90 | 45 | 7 | 1 | 58 | 60 | 29047 | – |
| **5** | Ar | EtOH/$H_2O$[b)] | 1.0% $Au/TiO_2$ | 11242 | 88 | 110 | 7 | 2 | 36 | 52 | 8258 | 182 |
| **6** | Ar | $H_2O$ | 1.0% $Au/TiO_2$ | 66 | – | – | – | – | – | – | – | – |
| **7** | $CO_2$ | EtOH | 0.45% $Au/TiO_2$ | 9930 | 51 | 34 | 1 | 1 | 13 | | 9258 | – |
| **8** | $CO_2$ | EtOH | 0.57% $Au/TiO_2$ | 11427 | 55 | 33 | 3 | – | 16 | | 10757 | – |
| **9** | $CO_2$ | EtOH | 1.0% $Au/TiO_2$ | 15402 | 95 | 62 | 3 | 1 | 29 | | 15235 | – |
| **10** | $CO_2$ | EtOH | 1.7% $Au/TiO_2$ | 18453 | 88 | 72 | 4 | 1 | 35 | | 17576 | – |

[a)]Stirred suspensions of the photocatalyst (25 mg) in the specified solvent (25 mL) were irradiated with a Hg lamp (125 W) under atmospheres of the specified gas (1.4 bar) at 25 °C for 2 h; hyphens denote figures lower than the corresponding detection limits; [b)]Ethanol/water at a 50:50 volume ratio.

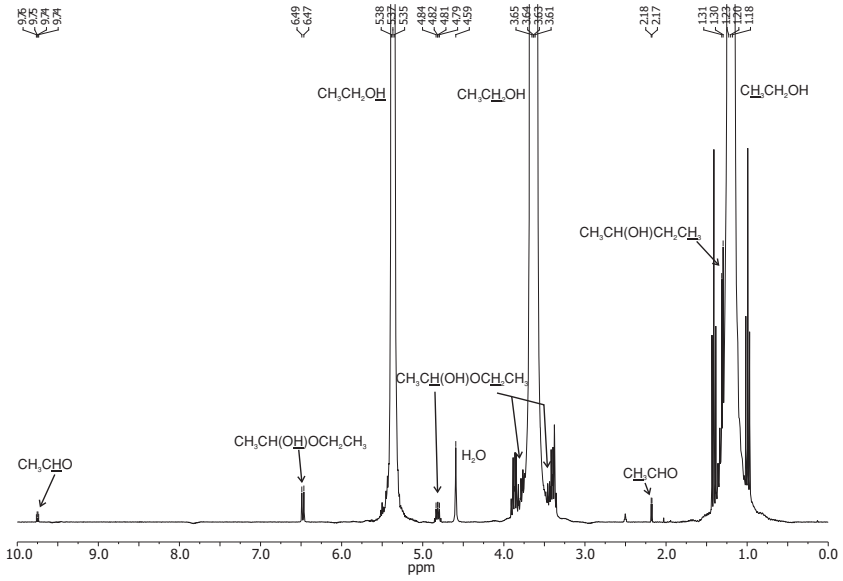


**Figure 5.** $^1$H NMR spectrum (300.13 MHz, 25 °C, dmso-$d_6$ as external reference) of a sample of the liquid phase after reaction **2** (see Table 1, 125 W Hg lamp irradiation of an ethanolic suspension of 0.57% Au/$TiO_2$ under 1.4 bar of Ar at 25 °C for 2 h). The signals of ethanol are off the scale; those for 1-ethoxyethane and acetaldehyde could be unambiguously assigned, as indicated on the spectrum.

order: $H_2$ >> $CH_4$ > CO > $C_2H_4$ > $CO_2$ > $C_2H_6$ > $C_3H_8$. Very high production rates (21–30 mmol $g_{cat}^{-1}$ $h^{-1}$) were observed for $H_2$, a fact which caused rapid pressure increases. To put these values into context, it should be commented that it has been recently reported that $H_2$ can be obtained from pure ethanol on Au/$TiO_2$ photocatalysts by illumination with 350 nm "black" light at ca. 5 or 12 mmol $g_{cat}^{-1}$ $h^{-1}$ (as estimated from data in references [14a] or [14b]). Based on a different approach, $H_2$ was produced from ethanol/water mixtures on glass-supported Pt/$TiO_2$ with 300–400 nm "black" light irradiation at a maximum rate of ca. 11 mmol $g_{cat}^{-1}$ $h^{-1}$ (when using a 80:20 ethanol:water volume ratio).[9] By using a Hg lamp (500 W) as the light source, $H_2$ production rates up to 6 or 10 mmol $g_{cat}^{-1}$ $h^{-1}$ were achieved from ethanol/water mixtures on Au/$TiO_2$ or Pt/$TiO_2$, respectively.[4] Similar results have also been reported by using methanol instead of ethanol.[16,17] Therefore, the data reported herein represent between two- and three-fold increases in $H_2$ production efficiency over state-of-the-art methods, with the exception of one reaction performed on a $RuO_2$-$TiO_2$-Pt photocatalyst, which proved extremely active, yielding $H_2$ at a 30 mmol $g_{cat}^{-1}$ $h^{-1}$ rate from a methanol/water (1:1 by volume) mixture using a 500 W Hg lamp.[3]

It is interesting to note that $H_2$ accounts for >99% (in moles) of all gases produced, which means that an almost pure $H_2$ stream could be potentially obtained by this method. Among the remaining gaseous products, ca. 0.5% of hydrocarbons were found. The highest production rate of $CH_4$ on Au/$TiO_2$ measured by us (up to 109 μmol $g_{cat}^{-1}$ $h^{-1}$, reaction **3** in Table 1) is higher than previously reported on similar catalysts (80 μmol $g_{cat}^{-1}$ $h^{-1}$),[4] but lower than that observed on Pt/$TiO_2$ analogues (180 μmol $g_{cat}^{-1}$ $h^{-1}$).[4]

In addition to the gaseous products, quantification of products in the liquid phase was also undertaken. In most cases, acetaldehyde was the only product found. Occasionally, smaller amounts of acetic acid were also generated. In fact, the acetaldehyde produced in the liquid phase occurs mainly as the hemiacetal formed by addition of one equivalent of ethanol, i.e. 1-ethoxyethanol, as inferred from $^1$H and $^{13}$C NMR analyses (see **Figure 5**). Integration of the $^1$H NMR signals allowed the quantification of each compound. For reaction **2**, the amounts of 1-ethoxyethanol and acetaldehyde were 1012 and 95 μmol, respectively. Such data (considering both free acetaldehyde and its hemiacetal, 1-ethoxyethanol) are consistent with those found by chromatographic analyses within less than ±9% error. The corresponding acetal, i.e. 1,1-diethoxyethane was not detected.

The amounts of acetaldehyde in the liquid phase are remarkably close to the stoichiometric amounts of $H_2$ determined in the gas phase (Table 1). This is consistent with the dissociation of ethanol into $H_2$ and acetaldehyde via reduction and oxidation reactions, respectively; as widely accepted, these reactions are enabled by electrons and holes photo-generated on the photocatalyst surface.[1,14b] The reactions can be summarised as follows:

$$CH_3CH_2OH + 2h^+ \rightarrow CH_3CHO + 2H^+ \quad (1)$$

$$2H^+ + 2e^- \rightarrow H_2 \quad (2)$$

where $h^+$ and $e^-$ represent the holes and electrons, respectively, generated on the photocatalysts by light absorption. Furthermore, the reaction

$$CH_3CHO + CH_3CH_2OH \rightarrow CH_3CH(OH)OCH_2CH_3 \quad (3)$$

takes place in the liquid phase leading to 1-ethoxyethanol, as discussed above.

Since $H_2$ and acetaldehyde are formed in molar ratios near the unity and their production rates are considerably larger than those of the other products detected, it seems reasonable to conclude that the predominant primary reactions in this system are those defined by Equations (1) and (2).

The effect of the composition of the solvent was studied by performing reactions either with water as a co-solvent or in pure water. Experiments carried out in ethanol/water mixtures (50:50 by volume) also yielded $H_2$ as the major gaseous product, although at noticeably lower rates; for example, ca. 28.5 vs. 11.2 mmol $g_{cat}^{-1}$ $h^{-1}$ were produced on 1.0% Au/$TiO_2$ under either pure ethanol or ethanol/water (reactions **3** and **5** in Table 1), respectively. Other production rates also diminished for reactions with water as a co-solvent, with the exception of that for ethylene, which increased from 45 to 110 μmol $g_{cat}^{-1}$ $h^{-1}$ (reactions **3** and **5** in Table 1). Irradiation of a suspension of 1.0% Au/$TiO_2$ in pure water yielded $H_2$ at a rate three orders of magnitude lower (66 μmol $g_{cat}^{-1}$ $h^{-1}$, reaction **6** in Table 1) than in ethanol. Not surprisingly, no carbon containing products were generated in water.

### 2.3. Photocatalytic Reforming of Ethanol Under $CO_2$

The photocatalytic reactions described above were performed under Ar atmosphere, in order to avoid the presence of air. Indeed, the production of $H_2$ was very fast, as shown in the previous section. Furthermore, the photocatalytic reduction of $CO_2$ on aqueous semiconductor suspensions has been widely investi gated,[2a,18] although the reported conversion rates are generally low (in the order of micromoles per gram of catalyst per hour). In most cases, a sacrificial electron donor is used to enhance yields. Among these, methanol is frequently chosen, although it has been demonstrated that it leads to products (mostly HCHO and $HCO_2H$) which may in part interfere with the analysis of $CO_2$ reduction products or intermediates.[18b,19] In the case reported here, ethanol also has a strong tendency to be oxidised (to acetaldehyde), and $H_2$ is produced in the coupled reduction reaction under Ar.

We were interested to know whether ethanol oxidation could be coupled with $CO_2$ reduction and how this process would affect the rate of $H_2$ evolution. The results obtained for the photocatalytic $H_2$ generation under UV-rich irradiation in the presence of $CO_2$ are summarised in Table 1. In fact, production rates for all products were noticeably lower under $CO_2$ atmosphere as compared to those found under Ar. For example, reactions on 1.0% $Au/TiO_2$ with Hg lamp light yielded $H_2$ at ca. 28.5 or 15.4 mmol $g_{cat}^{-1}$ $h^{-1}$ under Ar or $CO_2$ atmospheres (reactions **3** and **9** in Table 1), respectively, which translates into a 46% reduction in activity under $CO_2$. Acetaldehyde yields (matching those for $H_2$, as observed for reactions under Ar) diminished to a similar extent (see Table 1). This implies that $CO_2$ might be inhibiting the primary reactions (Equations (1) and (2)). Production rates of $CH_4$ and CO also decreased when performing the reactions under $CO_2$ instead of Ar. However, the decrease in $CH_4$ yield is lower than that of $H_2$; for example, only a 13% lower production yield was found for reactions on 1.0% $Au/TiO_2$ (from 109 to 95 μmol $g_{cat}^{-1}$ $h^{-1}$ under Ar or $CO_2$, respectively, see Table 1). Moreover, no further C1 products ($HCO_2H$, HCHO or $CH_3OH$) were detected by either GC or HPLC analyses of the liquid phases. Therefore, there is no clear evidence for significant conversion of $CO_2$ to C1 oxygenates. Consistent with these findings, no products were detected by $^{13}C$ NMR analysis of the liquid phase after irradiation (Hg lamp) of an ethanolic suspension of 0.57% $Au/TiO_2$ under a $^{13}CO_2$ atmosphere. The only noticeable positive influence of the presence of $CO_2$ in the photocatalytic irradiation was a slight increase in the amounts of ethylene, e.g. production rates of 45 or 62 μmol $g_{cat}^{-1}$ $h^{-1}$ (reactions **3** and **9** in Table 1) were found under Ar or $CO_2$ atmospheres on 1.0% $Au/TiO_2$, respectively.

### 2.4. Effect of Gold Loading

The effect of gold loading on the activity of the photocatalysts can be seen in Table 1 and **Figure 6**. The production of $H_2$ increased with increasing gold loading. For example, $H_2$ production rates under Ar were ca. 23.2 or 28.5 μmol $g_{cat}^{-1}$ $h^{-1}$ (a 23% increase) for 0.45 or 1.0% Au contents (reactions **1** and **3** in Table 1), respectively. For reactions under $CO_2$ atmosphere, the effect is even more noticeable: The yield of $H_2$ was 55% higher by increasing gold loading from 0.45 or 1.0% (see Table 1 and Figure 6). This trend agrees with recent studies which correlate $H_2$ production with the availability of surface gold atoms at the interface with $TiO_2$.[14b] Similar effects were found for the amounts of acetaldehyde produced and for the rest of the minor gaseous products. Therefore, it appears that the photocatalytic activity increases in general with gold loading.

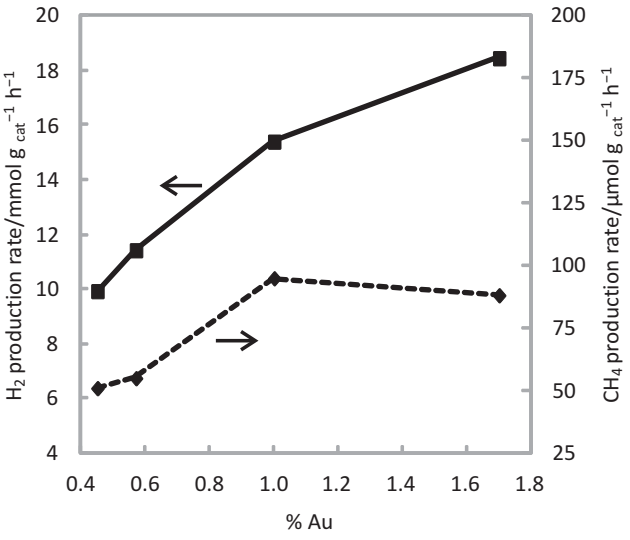


**Figure 6.** Production of $H_2$ and $CH_4$ from ethanol vs. gold loading (wt%) on $Au/TiO_2$ solids. The reactions were performed by irradiating (Hg lamp, 125 W) a suspension of the photocatalyst (25 mg) in ethanol (25 mL) under a $CO_2$ atmosphere (1.4 bar) for 2 h. Note the two orders of magnitude difference between both vertical axes ($H_2$ and $CH_4$ production rates, left and right, respectively).

### 2.5. Control Experiments: Photolysis without Catalysts

Aiming at both proving the activity of the photocatalysts and investigating on the mechanistic origin of the products, control experiments without any catalyst were performed. As shown in **Table 2**, after irradiation of ethanol in the absence of $Au/TiO_2$ solids, several products ($H_2$, $CH_4$, $C_2H_4$ or $C_2H_6$) were formed; nevertheless, their amounts were smaller by two to three orders of magnitude as compared to those obtained from catalysed reactions. Thus, only 3.06 μmol of $H_2$ were produced from the non-catalysed irradiation (Hg lamp) of ethanol for 2 h, whereas an analogous reaction in the presence of 1.0% $Au/TiO_2$ yielded ca. 1421 μmol, i.e., an amount 465 times larger. The productions of $CH_4$ were 0.12 and 5.44 μmol (reactions **11** and **3** in Table 2), without or with 1.0% $Au/TiO_2$, respectively, which means an increase by a factor of 45 by use of the photocatalyst. On the other hand, only trace amounts of CO were produced without the photocatalyst. The amount of $CO_2$ was only marginally smaller for the non-catalysed irradiation (0.64 μmol) than for the analogous experiment on 1.0% $Au/TiO_2$ (1.11 μmol). Traces of acetaldehyde were also detected in the liquid phase of experiments without catalyst, but unfortunately, the low amounts formed makes accurate quantification difficult.

The formation of small amounts of $H_2$, $CH_4$ or $C_2H_6$ solely by the action of light might be ascribed to several reactions

**Table 2.** Product yields (in micromoles) for the UV-rich light irradiation of ethanol with or without photocatalysts.[a)]

| | Gas | Photocatalyst | Produced amount [μmol] | | | | | | | | |
|---|---|---|---|---|---|---|---|---|---|---|---|
| | | | Gas phase | | | | | | | Liquid phase | |
| | | | $H_2$ | $CH_4$ | $C_2H_4$ | $C_2H_6$ | $C_3H_8$ | CO | $CO_2$ | $CH_3CHO$ | $CH_3COOH$ |
| **11** | Ar | – | 3.06 | 0.12 | 0.02 | 0.03 | – | 0.01 | 0.64 | – | – |
| **12** | $CO_2$ | – | 5.24 | 0.17 | 0.03 | 0.06 | – | 0.07 | | – | – |
| **3**[b)] | Ar | 1.0% Au/$TiO_2$ | 1421.38 | 5.44 | 2.24 | 0.35 | 0.05 | 2.82 | 1.11 | 1401.05 | – |
| **9**[b)] | $CO_2$ | 1.0% Au/$TiO_2$ | 675.87 | 3.77 | 3.12 | 0.17 | 0.06 | 1.60 | | 728.93 | – |

[a)]Stirred suspensions of the photocatalyst (25 mg) in ethanol (25 mL) were irradiated with a Hg lamp (125 W) under atmospheres of the specified gas (1.4 bar) at 25 °C for 2 h; hyphens denote figures lower than the corresponding detection limits; [b)]Note that data for reactions **3** and **9**, also reported in Table 1, are included here for comparison.

involving radicals, as previously reported for the low temperature photolysis of ethanol.[20] In the presence of 1.0% Au/$TiO_2$, the fact that the production rates of $H_2$ and acetaldehyde were greatly enhanced (vide supra) is in agreement with the reduction and oxidation reactions stated in Equations (1) and (2). The case of $CH_4$ or $C_2H_6$, the yields of which are also enhanced, although to a lesser extent (see Table 2), is less obvious; they might be produced from radical reactions (similar to those suggested in ref. [20]) promoted by photo-generated electrons and holes on the gold-titania solids. On the other hand, the small amounts of ethylene detected could be a result of either ethanol dehydration or free radical reactions.

In summary, the results from control experiments indicate that direct photolysis has little influence on the conversion of ethanol, confirming that Au/$TiO_2$ materials are highly active for the production of (mainly) $H_2$ by photoreforming, and that the presence of $CO_2$ has a negative influence on the performance of this process.

### 2.6. Photoreactions under Simulated Solar Light

The process of ethanol photoreforming presented here would have significant practical interest if it could be carried out under solar radiation as the only energy source. In order to prove the efficiency of this photocatalytic reforming, reactions were carried out under simulated solar light.

The data in **Table 3** reveal that $H_2$ is the main gaseous product from simulated solar light irradiations of ethanolic Au/$TiO_2$ suspensions under Ar. Minor products were $CH_4$, $CO_2$ and $C_2H_4$; interestingly, the production of CO is immeasurable (or at trace levels) in most cases. The $H_2$ production rates were in the 5.2–6.2 mmol $g_{cat}^{-1}$ $h^{-1}$ range, that is, between one third and one fifth of those found under Hg lamp illumination. However, the molar (or volume) proportion of $H_2$ relative to the entirety of gaseous products is still extremely high. The selectivity towards $H_2$ is > 99.3% (reactions **13** and **14** in Table 3), slightly higher than for UV-richer irradiations. The production yields of $CH_4$ and $C_2H_4$ are also significantly lower than those found under Hg lamp light (84% and 76% decreased yields, respectively, for 1.0% Au/$TiO_2$ suspensions under Ar, reactions **3** and **14** in Table 1 and Table 3). The stoichiometry of the reactive system under simulated solar light is in agreement, as previously hypothesised for UV-richer irradiations, with Equations 12, since acetaldehyde yields match those of $H_2$ within a maximum error of ±10%. It is worth noting that, albeit only modestly, the production of $CH_4$ and $C_2H_4$ increased when performing the reactions under $CO_2$ instead of Ar. For example, $C_2H_4$ was formed at 22 or 11 μmol $g_{cat}^{-1}$ $h^{-1}$ rates on 1.0% Au/$TiO_2$ under $CO_2$ or Ar atmospheres (reactions **16** and **14** in Table 3), respectively.

The above results indicate that an ethanol photoreforming process using solar irradiation as the energy source might be envisaged. Moreover, the somewhat higher $H_2$ selectivities

**Table 3.** Product yields for the photocatalytic ethanol reforming under simulated solar light on Au/$TiO_2$.[a)]

| | Gas | Photocatalyst | Production rate [μmol $g_{cat}^{-1}$ $h^{-1}$] | | | | | | | | |
|---|---|---|---|---|---|---|---|---|---|---|---|
| | | | Gas phase | | | | | | | Liquid phase | |
| | | | $H_2$ | $CH_4$ | $C_2H_4$ | $C_2H_6$ | $C_3H_8$ | CO | $CO_2$ | $CH_3CHO$ | $CH_3COOH$ |
| **13** | Ar | 0.45% Au/$TiO_2$ | 5919 | 13 | 8 | – | – | – | 17 | 6175 | – |
| **14** | Ar | 1.0% Au/$TiO_2$ | 6151 | 17 | 11 | – | – | – | 12 | 6522 | – |
| **15** | $CO_2$ | 0.57% Au/$TiO_2$ | 5539 | 38 | 25 | – | – | – | | 5317 | – |
| **16** | $CO_2$ | 1.0% Au/$TiO_2$ | 5219 | 26 | 22 | – | – | 1 | | 5843 | – |

[a)]Stirred suspensions of the photocatalyst (25 mg) in ethanol (25 mL) were irradiated with simulated solar light (100 mW $cm^{-2}$) under atmospheres of the specified gas (1.4 bar) at 25 °C for 2 h; hyphens denote figures lower than the corresponding detection limits.

observed as compared to those found for Hg lamp irradiation experiments, represent another important advantage regarding the use of solar light. Such higher selectivities could be due to a lesser extent of ethanol and/or acetaldehyde photolysis yielding, inter alia, $CH_4$ and CO as undesired gaseous products. Therefore, yield and selectivity may be further optimised by judiciously adjusting irradiation wavelength limits and extending on the systematic exploration of relevant $Au/TiO_2$ photocatalyst characteristics (e.g. Au loading, Au particle size or $TiO_2$ crystalline phase composition). Eventually, a high performance continuous process for $H_2$ production from ethanol under sun light might be designed.

## 3. Conclusions

Catalysts consisting of gold nanoparticles deposited on the surface of anatase-rich titania ($Au/TiO_2$), prepared by a simple deposition-precipitation method, proved to be extremely active for the photoreforming of ethanol under UV-rich (Hg lamp) light. The main products of such processes were $H_2$ in the gas phase and acetaldehyde in the liquid phase, both obtained according to the reaction $CH_3CH_2OH \rightarrow CH_3CHO + H_2$, promoted by the photo-generated electrons and holes on the photocatalysts. Production rates for $H_2$ were around 30 mmol $g_{cat}^{-1}$ $h^{-1}$ on 1.7% $Au/TiO_2$, with a volumetric proportion of $H_2$ in the mixture of gas phase products exceeding 99%, the remaining components being hydrocarbons, such as $CH_4$, $C_2H_4$ or $C_2H_6$, and minor amounts of CO and $CO_2$. Experiments under simulated solar light revealed that, although at lower yields than under UV irradiation, significant amounts of $H_2$ (5–6 mmol $g_{cat}^{-1}$ $h^{-1}$) were also produced by the photoreforming of ethanol. The selectivity towards $H_2$ was even improved (>99.3%) under simulated solar light, probably because of its lower UV irradiation intensity, and therefore, lesser extent of photolytic reactions. Such results are in agreement with previous reports using $Au/TiO_2$ as photocatalysts for $H_2$ generation under other conditions and hold promise regarding the design of a process by which almost pure $H_2$ would be produced from a cheap, biomass-derived feedstock, such as ethanol, with the Sun as the only energy source.

## 4. Experimental Section

*Materials*: Titanium dioxide (Aeroxide P25) was kindly supplied by Evonik Degussa. Hydrogen tetrachloroaurate(III) hydrate ($HAuCl_4{\cdot}3H_2O$) was supplied by Sigma-Aldrich. Absolute ethanol (Multisolvent HPLC grade) and sulfuric acid (95–97%, synthesis grade) were supplied by Scharlau. Sodium hydroxide (pellets, 98%) was supplied by VWR. Carbon dioxide (≥99.995%) and argon (≥99.995%) were supplied by Abelló Linde.

*Photocatalyst Syntheses*: The $Au/TiO_2$ materials were prepared by deposition-precipitation methodologies. For example, to prepare ca. 1.0 g of 1.0% $Au/TiO_2$, $HAuCl_4{\cdot}3H_2O$ (19.99 mg) was added to ultrapure (Milli-Q) water (100 mL). The pH was brought to 9.0 by adding the appropriate amount of a 0.2 M aqueous NaOH solution. Once the pH reading had remained stable, $TiO_2$ (1.0 g) was added under stirring, and then the pH was adjusted to 9.0 again as described above. The obtained suspension was vigorously stirred overnight. The solid was collected by filtration and thoroughly washed with ultrapure (Milli-Q) water. After deposition, gold was thermally reduced by heating the sample at 300 °C under a $H_2$ atmosphere for 5 h, this process leading to the formation of gold nanoparticles.

*Photocatalyst Characterisations*: XRD measurements were performed by means of a PANalytical Cubix'Pro diffractometer equipped with an X'Celerator detector and automatic divergence and reception slits using Cu-$K_\alpha$ radiation (0.154056 nm). TEM images were taken on a Philips CM-10 instrument at a 100 kV accelerating voltage. Gold contents were determined by inductively coupled plasma (ICP) analyses performed on a Varian 715-ES ICP Optical Emission Spectrometer and by X-ray fluorescence by means of a PANalytical MiniPal4 spectrometer. UV-vis absorption spectra were recorded by diffuse reflectance UV-vis (DRUV-vis) spectroscopy on a Varian Cary 5000 UV-Vis-NIR Spectrophotometer.

*Photocatalytic Reactions*: In a typical experiment, the photocatalyst powder (25 mg) was suspended in ethanol (25 mL) by sonication for 15 min. The resulting suspension was then transferred to a cylindrical quartz reactor (diameter ≈ 44 mm, volume ≈ 50 mL, equipped with a gas inlet valve, a gas outlet valve and a pressure gauge) and purged with the desired gas (Ar or $CO_2$, 5 mL $min^{-1}$ for 15 min, and then pressurized-depressurised to 1.4 bar for five cycles); the reactor was finally loaded with the desired gas (1.4 bar) and tightly closed. The suspension was stirred (500 $min^{-1}$) and irradiated with either a medium pressure Hg lamp or a solar simulator. In the case of the Hg lamp (125 W), irradiation was performed from the top at a distance of ca. 6 cm between the light source and the suspension surface for the desired length of time; the reactor vessel was kept in a water bath at ca. 25 °C throughout the experiment. In experiments where simulated solar light (Abet Technologies Sun 2000 Solar Simulator) was used, the suspension was illuminated with a collimated light beam from the top at a distance of ca. 10 cm and the reactor kept in a water bath at 25 °C. After the light had been switched off, the reaction mixtures were stirred until the pressure reading had stabilised. Two different gaseous samples were taken through the outlet valve port: (*g1*) a 50 µL sample which was injected "on-column" on a gas chromatograph (Agilent Technologies 7890A GC System) equipped with a Mol Sieve 5 column (carrier gas: Ar, flow = 5 mL $min^{-1}$) and a thermal conductivity detector (TCD) for the quantification of $H_2$, $CH_4$ and CO; and (*g2*) a 50 mL sample which was injected on a three-channel chromatograph (Varian 450-GC Rapid Refinery Gas Analyser) equipped with one TCD for the quantification of $H_2$ (first channel), one TCD for the quantification of $CO_2$ and CO (second channel), and one flame ionisation detector (FID) for the quantification of $CH_4$, $C_2H_4$, $C_2H_6$ and $C_3H_8$ (third channel); the carrier gases were Ar (first channel) and He (second and third channels). The amounts of $H_2$, $CH_4$ and CO were averaged over the figures obtained by analyses of both gaseous samples (*g1* and *g2*), which agreed within a standard deviation of ca. 4%. Moreover, two different liquid samples, obtained from a centrifuged and decanted aliquot of the final suspension, were analysed as follows: (*l1*) a ca. 0.5 g sample was diluted with ultrapure water (ca. 4.5 g), acidified by addition of a 1.4 M aqueous $H_2SO_4$ solution (ca. 0.015 g), and analysed by liquid chromatography on a Coregel 87H column (Waters 1525 Binary HPLC Pump, injection volume = 10 µL, column temperature = 70 °C, eluent: 4 mM aqueous $H_2SO_4$, flow rate = 0.7 mL $min^{-1}$) and a refractive index detector (Waters 2410) for the quantification of acetaldehyde and acetic acid; and (*l2*) a liquid sample was injected without any further treatment (actual injection volume = 1 µL) on a gas chromatograph (Agilent Technologies 7890A GC System) equipped with a HP-5 column (carrier gas: He, flow rate = 1 mL $min^{-1}$) and a FID for the quantification of acetaldehyde. The reported amounts of acetaldehyde were averaged over the figures obtained by analyses of both liquid samples (*l1* and *l2*), which agreed within a standard deviation of ca. 8%. In some cases, the liquid phases of the final reaction mixtures (after separation of the catalyst) were analysed by $^1H$ and $^{13}C$ NMR spectroscopies (300.13 MHz and 75.48 MHz, respectively) spectroscopy at 25 °C on a Bruker Avance-300 spectrometer, using dimethyl sulfoxide-$d_6$ (dmso-$d_6$) inside a co-axial capillary tube as the reference solvent.

## Acknowledgements

This work has been supported by the JAE-Doc program, co-funded by the *Consejo Superior de Investigaciones Científicas* (CSIC) and the European

Social Fund (ESF). A.V.P. is grateful to CSIC for a JAE-Doc post-doctoral grant. Financial support by the *Generalitat Valenciana* (Prometeo 20/2/014) is gratefully acknowledged.

Received: June 4, 2013
Published online: August 1, 2013

[1] X. B. Chen, S. H. Shen, L. J. Guo, S. S. Mao, *Chem. Rev.* **2010**, *110*, 6503.
[2] a) Y. Izumi, *Coord. Chem. Rev.* **2013**, *257*, 171; b) S. C. Roy, O. K. Varghese, M. Paulose, C. A. Grimes, *ACS Nano* **2010**, *4*, 1259; c) M. Halmann, ÷lman, B. Aurian-Blajeni, *Sol. Energy* **1983**, *31*, 429.
[3] T. Kawai, T. Sakata, *J. Chem. Soc., Chem. Commun.* **1980**, 694.
[4] G. R. Bamwenda, S. Tsubota, T. Nakamura, M. Haruta, *J. Photochem. Photobiol. A—Chem.* **1995**, *89*, 177.
[5] a) G. W. Huber, S. Iborra, A. Corma, *Chem. Rev.* **2006**, *106*, 4044; b) D. M. Alonso, J. Q. Bond, J. A. Dumesic, *Green Chem.* **2010**, *12*, 1493.
[6] a) R. D. Cortright, R. R. Davda, J. A. Dumesic, *Nature* **2002**, *418*, 964; b) G. W. Huber, J. W. Shabaker, J. A. Dumesic, *Science* **2003**, *300*, 2075.
[7] T. Kawai, T. Sakata, *Nature* **1980**, *286*, 474.
[8] T. Sakata, T. Kawai, *Nouv. J. Chim.* **1981**, *5*, 279.
[9] N. Strataki, V. Bekiari, D. I. Kondarides, P. Lianos, *Appl. Catal. B-Environ.* **2007**, *77*, 184.
[10] A. Gallo, T. Montini, M. Marelli, A. Minguzzi, V. Gombac, R. Psaro, P. Fornasiero, S. V. Dal, *ChemSusChem* **2012**, *5*, 1800.
[11] T. Montini, V. Gombac, L. Sordelli, J. J. Delgado, X. Chen, G. Adami, P. Fornasiero, *ChemCatChem* **2011**, *3*, 574.
[12] Y. Mizukoshi, K. Sato, T. J. Konno, N. Masahashi, *Appl. Catal. B-Environ.* **2010**, *94*, 248.
[13] T. Sakata, T. Kawai, *Chem. Phys. Lett.* **1981**, *80*, 341.
[14] a) M. A. Nadeem, M. Murdoch, G. I. N. Waterhouse, J. B. Metson, M. A. Keane, J. Llorca, H. Idriss, *J. Photochem. Photobiol. A—Chem.* **2010**, *216*, 250; b) M. Murdoch, G. I. N. Waterhouse, M. A. Nadeem, J. B. Metson, M. A. Keane, R. F. Howe, J. Llorca, H. Idriss, *Nat. Chem.* **2011**, *3*, 489.
[15] a) A. Primo, A. Corma, H. García, *Phys. Chem. Chem. Phys.* **2011**, *13*, 886; b) M. A. Centeno, M. C. Hidalgo, M. I. Dominguez, J. A. Navío, J. A. Odriozola, *Catal. Lett.* **2008**, *123*, 198.
[16] M. Zalas, M. Laniecki, *Sol. Energy Mater. Sol. Cells* **2005**, *89*, 287.
[17] M. Buaki-Sogo, M. Serra, A. Primo, M. Alvaro, H. Garcia, *ChemCatChem* **2013**, *5*, 513.
[18] a) T. Inoue, A. Fujishima, S. Konishi, K. Honda, *Nature* **1979**, *277*, 637; b) A. Dhakshinamoorthy, S. Navalon, A. Corma, H. Garcia, *Energy Environ. Sci.* **2012**, *5*, 9217; c) V. P. Indrakanti, J. D. Kubicki, H. H. Schobert, *Energy Environ. Sci.* **2009**, *2*; d) S. Navalón, A. Dhakshinamoorthy, M. Álvaro, H. Garcia, *ChemSusChem* **2013**, *6*, 562; e) S. N. Habisreutinger, L. Schmidt-Mende, J. K. Stolarczyk, *Angew. Chem.-Int. Ed.* 2013, 52, 7372.
[19] N. Ulagappan, H. Frei, *J. Phys. Chem. A* **2000**, *104*, 7834.
[20] H. S. Judeikis, S. Siegel, *J. Chem. Phys.* **1965**, *43*, 3625.